01 Jan 2015

Thevenin Equivalence in Disorderless Quantum Networks

C. A. Cain

Cheng-Hsiao Wu

Missouri University of Science and Technology, chw@mst.edu

Thévenin equivalence in disorderless quantum networks

C. A. Cain and C. H. Wu[a)]
Department of Electrical and Computer Engineering, Missouri University of Science and Technology, 301 W 16th St., Rolla, Missouri 65409, USA

(Received 28 August 2014; accepted 26 December 2014; published online 13 January 2015)

We outline the procedure of extending the Thévenin equivalence principle for classical electric circuits to reducing Aharonov-Bohm-based quantum networks into equivalent models. With examples, we show from first principles how the requirements are related to the electron band structure's Fermi level and the lattice spacing of the network. Quantum networks of varying degrees of coupling strength from four basic classifications of single and double entangled loops sharing symmetry and highly correlated band structures are used to demonstrate the concept. We show the limitations of how the principle may be applied. Several classes of examples are given and their equivalent forms are shown. © *2015 AIP Publishing LLC*.
[http://dx.doi.org/10.1063/1.4905691]

I. INTRODUCTION

Quantum networks in the mesoscopic range have been well-studied over the last few decades,[1–12] with more recent work focusing on higher-order effects and topics such as spin transport due to their potential development for quantum computation.[13–24] Quantum networks consist of quasi-one-dimensional paths and nodes connected together. Because of the existence of loops, the Aharonov-Bohm (AB) effect can be applied to further modulate the phase of the electron wavefunction along the paths where Schrödinger's equation is satisfied. Over the last few years, we have been investigating the behavior when a few AB rings are coupled for quantum computing.[25–27] For this purpose, it is important to identify whether these quantum networks have the potential to replace conventional electric circuits with new ones based on the phase-modulation concept.

One area that has yet to be explored for these complex quantum networks is the concept of equivalence. In classical circuits, such as the simple resistive network shown in Fig. 1(a), Léon Thévenin famously showed in the 1800s that it is possible to form a simpler equivalent version for part of the circuit.[28] The simplified network preserves the total current and voltage difference being delivered to the unaltered part of the circuit. This has long been a useful analysis tool in simplifying complex electronic designs to better understand their behavior. We have recently shown a quantum network-based processor utilizing symbolic substitution rules, not superposition of flux qubits.[29] Therefore, the question of extending Thévenin's theorem to quantum networks becomes an important means for simplification and gaining physical insight about them. For a general classic circuit, the system is lossy and the transport is incoherent. Thus, when forming an equivalent circuit, the equivalent current being delivered to the unaltered part of the circuit in both models will be a scalar. However, at the mesoscopic level, where ballistic transport and elastic scattering are possible, the quantum circuits take into effect the magnitude and phase of the electron wavefunction in relation to the band structure and chemical potential. These can obviously differ between the original and equivalent models. In this work, we attempt to determine how these restrictions affect the possibility of finding such equivalent networks.

The remainder of the paper is divided into three parts. Section II will define a quantum network and its properties as well as outline the analytical model used in our calculations. Section III is divided into three subsections, with the first (Sec. III A) describing the general requirements that need to be met between two networks in order to satisfy an equivalence. Secs. III B and III C focus on determining which specific quantum networks can meet these criteria based on their coupling strength. Finally, the results and observations are summarized in Sec. IV.

II. PHYSICAL MODEL AND CALCULATION METHOD

Electron transport in AB-modulated networks can be modeled in a multiply connected space of uniform quasi-1D paths of length l interconnected by M nodes. It is placed between two thermal reservoirs with a small chemical potential difference $\mu_H - \mu_L$ at infinity, which acts as the source and sink of the electron. There is also an external magnetic flux Φ present, as shown in Fig. 2. In these quantum networks, the well-known Landauer-Büttiker formula for conductance applies between any two points in the network. In Fig. 2, nodes A and C are the elastic scatterers. The system's transport can be tuned by modifying the flux inside the loop, which alters the phase of the electron wavefunction within the paths. The transport between any two points i and j needs to satisfy the Büttiker symmetry principle $T_{ij}(\Phi) = T_{ji}(-\Phi)$.[30,31]

A brief formulation of the model will be presented here, with a more complete description given in previous work.[32] The Schrödinger equation must be satisfied at any point in the ring. For a single free electron situation, the solution between nodes A and B can be given as

$$\Psi_{AB}(x) = [P_{AB}e^{-ikx} + Q_{AB}e^{ikx}]e^{-iS(x)/\hbar}, \tag{1}$$

where $\Psi_{AB}(0) = \Psi_{AB}(A)$, and $\Psi_{AB}(l) = \Psi_{AB}(B)$. P_{AB} and Q_{AB} are the complex outgoing and incoming wave

a)Electronic mail: chw@mst.edu

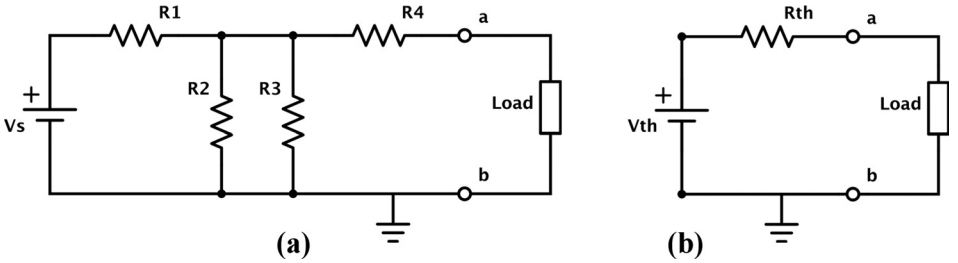

FIG. 1. (a) Simple resistor network with a voltage source *Vs* driving a load connected at terminals *a* and *b*. (b) Thévenin equivalent model that delivers an equal current through the terminals *a* and *b* to the same unaltered load. *Vth* is the open circuit voltage of the original network without the load connected, and *Rth* is the equivalent output resistance.

amplitudes from A in the path, respectively. S is a phase factor introduced due to the magnetic vector potential $\mathbf{A}$ and is given by the path integral

$$S(x)/\hbar = \frac{e}{\hbar c}\int_0^x \mathbf{A}(x')\cdot d\mathbf{x}' = \frac{x}{r}\left[\frac{\Phi}{\Phi_0}\right], \tag{2}$$

where x/r is the angular displacement and the elementary flux quantum $\Phi_0 = hc/e$. A is connected to a total of three nodes: B, D, and I. A simplified set of equations can then be formed as

$$\begin{aligned}\Psi(B) &= \Psi(A)[\cos kl - \tan\delta_{AB}\sin kl]e^{-i\phi},\\ \Psi(D) &= \Psi(A)[\cos kl - \tan\delta_{AD}\sin kl]e^{i\phi},\\ \Psi(I) &= \Psi(A)[\cos kl - \tan\delta_{AI}\sin kl],\end{aligned} \tag{3}$$

where $\phi = (2\pi/M)(\Phi/\Phi_0)$. For a neighbor node j, $\tan\delta_{Aj} = i\frac{P_{Aj}-Q_{Aj}}{P_{Aj}+Q_{Aj}}$ and the reflection coefficient $R_{Aj} = (P_{Aj}/Q_{Aj})$. Conservation of probability current requires $\sum_j \tan\delta_{Aj} = 0$, and allows one to reduce the set of Eq. (3) into a single node equation for A as

$$\Psi(A)[2\cos kl + \tan\delta_{AI}\sin kl] - e^{i\phi}\Psi(B) - e^{-i\phi}\Psi(D) = 0. \tag{4}$$

A similar node equation can be found for the other three nodes in the ring. To calculate the energy spectrum, the isolated system is considered first (no terminals). This fixes $\tan\delta_{AI} = 0$ in Eq. (4). The secular determinant for the four node equations becomes

$$16\cos^4 kl - 16\cos^2 kl - 2\cos 4\phi + 2 = 0. \tag{5}$$

The four possible energy states $E_n = k_n^2(h^2/8\pi^2 m)$ can then be found, with m being the electron mass. The half-filled Fermi energy state E_F at $T = 0\,\mathrm{K}$ is then used to solve for the

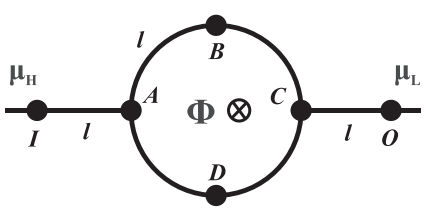

FIG. 2. Single symmetric two-terminal AB ring consisting of four nodes and lattice spacing l, placed between terminals of chemical potential difference $\mu_H - \mu_L$. H and L are the higher and lower potentials, respectively. A magnetic flux Φ penetrates the loop, adding an additional phase factor to the electron wavefunction. At each node (A,B,C,D), there is an associated node equation that relates the wavefunctions between other adjacent nodes.

transport. The terminals are considered a perturbation to the system, leading to the transmission and reflection coefficients. This is consistent with the S-matrix results first reported by Büttiker *et al.*[10] We have used this method to study more complicated AB ring configurations in the past.[33,34]

III. THÉVENIN EQUIVALENCE

A. Requirements

There are four basic classes of AB rings, determined by the number of M nodes in the ring: $M = 4N$, $4N+2$, $4N+1$, and $4N+3$, with N an integer. More complicated quantum networks can then be formed by coupling these AB rings together with different strengths and attaching several terminals. The key question is "Under what circumstances can these quantum networks be simplified like the classical circuit example in Fig. 1?" Clearly, if the state of a system and its equivalent form need to be identical at a node, significant restrictions will be imposed. The band structure becomes the first factor in determining whether or not a given network can be substituted for another. The scaling relations for the transport in AB rings investigated previously provide some insight.[26] For a symmetric ring such as the example in Fig. 2, it is possible to scale the network by any integer factor and still preserve the general band structure and hence the transport. The Fermi energy E_F and wavevector k_F for both structures are identical. When attempting to replace a portion of a quantum network with a simplified equivalent form, the node equations (as in Eq. (4)) for the unaltered portion of the network need to be identical. Due to these requirements, the correlation between the band structures of two different networks needs to be strong but not necessarily identical. In general, they will need to share some form of symmetry. Also, the correlation depends on the strength of the coupling between the AB rings. Ideally, E_F should be equal across the entire flux period to have the highest likelihood of satisfying the equivalence. This is satisfied by point-contact coupled rings and will be shown first in Sec. III B. It and Sec. III C are divided by coupling strength for the four basic classes of coupled AB rings.

B. Point-contacted loops

Point-contacted AB loops are a suitable starting point to demonstrate Thévenin equivalence. They share an identical band structure with a single ring, only with extra flux-invariant states added. Even though the Fermi energies are equal, it is not possible to meet the equivalence conditions

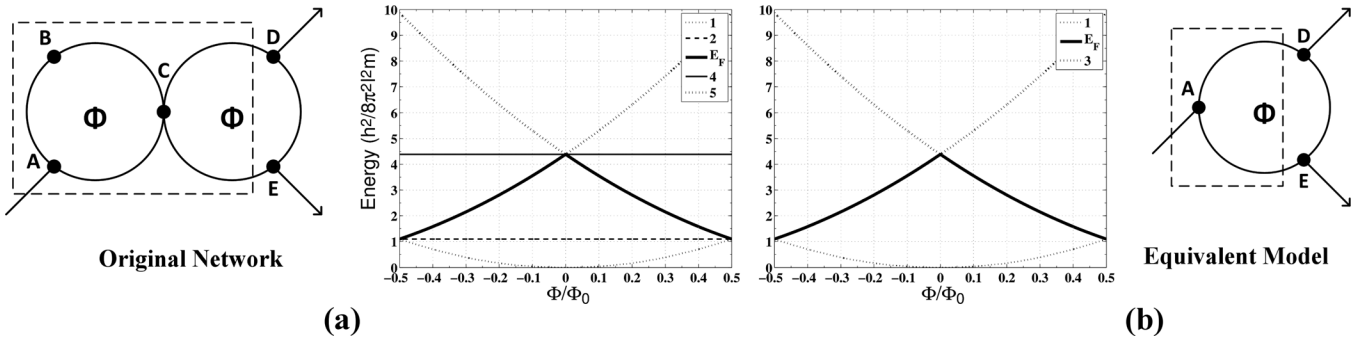

FIG. 3. (a) Network diagram and energy band structure (in units of $h^2/8\pi^2l^2m$) for two $M=3$ point-contacted loops. The dashed portion of the network will be replaced with an equivalent form shown in (b). The output nodes D and E remain unchanged. The lines in the band diagrams correspond to the energy states computed from the secular determinants of each network, similar to that of Eq. (5). Note that in (a), there are five nodes and thus five energy states, two of which are flux invariant. In (b), there are three nodes and three energy states, which are identical to the flux dependent states in (a). The Fermi energies E_F for both networks are aligned across the entire flux period.

across the entire flux range. We show that an equivalent circuit is only possible at a pair of flux values. Beginning with a network consisting of odd point-contacted $M=3$ rings belonging to the $4N+3$ class, shown in Fig. 3, it can be shown that its Fermi energy is equivalent to that of a single ring. This is due to the symmetry of the structure, though the point-contact causes the transmission to be compressed into a narrower flux range due to a resonant tunneling effect.

If three terminals are attached, as shown in Fig. 3(a), a Thévenin equivalent can be given in Fig. 3(b), where the left portion of the network is replaced with a single odd three-terminal ring. This happens to be a quantum circulator.[33] The wavefunction magnitudes for nodes D and E in both networks are shown in Fig. 4, with peaks at $|\Phi| = \Phi_0/4$ with Fermi wavevector $k_F = \pi/2l$. This value leads to the $\cos kl$ term in Eq. (4) vanishing at each node. The two node equations at B and C in the original network now only contain phase terms between the wavefunctions at adjacent nodes. The remaining three node equations take on a similar form of the equivalent single ring. The preserved part of the network does not necessarily have to contain two output terminals. For instance, if either one of the output terminals were removed to form a simpler two-terminal network, the Thévenin conditions would still hold. The wavefunctions at D and E between the two networks do however vary by a constant phase factor $\theta = \pi/3$. This can be offset by preparing the incident electron with a phase of θ to align the two network states. This means the inputs for the two equivalent networks need to differ by θ in phase space to obtain complete equivalence. Note that by scaling the number of nodes M in both rings by any odd integer, the same equivalence can be maintained.

The second example is the $M=4N+1$ class. The point-contacted $M=5$ AB rings are shown for the two-terminal situation in Fig. 5(a). It is possible to replace the left side of the network with the smaller equivalent form of a single loop. In this case, four nodes (E,F,G,H) are in the unaltered part of the network, one being the output terminal. The Fermi energy levels between the two networks are identical across the entire flux period. The Thévenin condition is again satisfied at $|\Phi| = \Phi_0/4$.

However, for the even-numbered $4N$ or $4N+2$ class, it is not possible to satisfy the equivalence requirements since their Fermi levels are independent of the applied flux. The

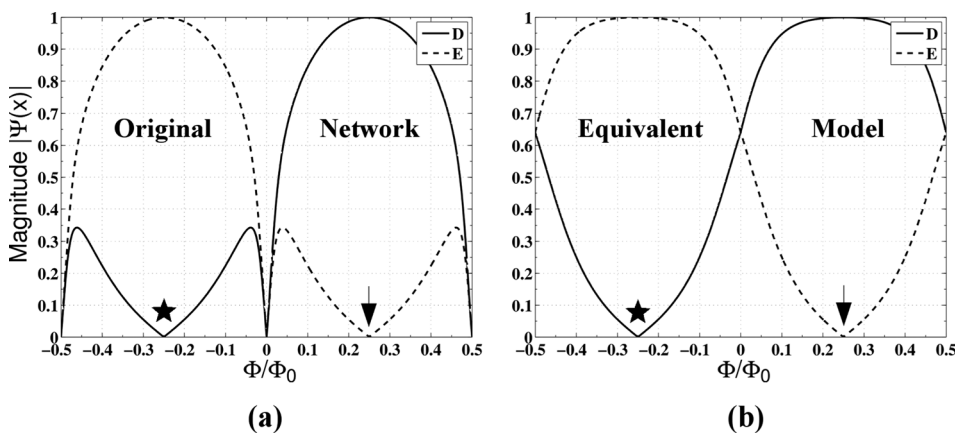

FIG. 4. Wavefunction magnitude of outputs D and E for the point-contacted network and its equivalent model given in Fig. 3. While the Fermi energies are equivalent across the entire period, the equivalence conditions are only met at two flux values $|\Phi| = \Phi_0/4$. This is indicated by the pair of arrows and stars, with corresponding energy $E = h^2/32l^2m$. This is because the $\cos kl$ terms vanish in the node equations since the Fermi wavevector $k_F = \pi/2l$. There is a phase shift of $\pi/3$ rad between the two networks for both flux values at nodes D and E. To obtain complete equivalence, the inputs at A in both networks need to differ by this constant phase.

incident electron is totally reflected to the input terminal, which does not occur for even-numbered, single rings. Therefore, none of the Thévenin conditions are satisfied other than sharing the same lattice spacing l.

C. Stronger coupled loops

There are two types of stronger coupling: the loops can share a single scattering path, or they can share two. A single path is the strongest form. For a single path in each of the four classes, the energy states that form the band structures are distorted from those of a single ring. Another issue that complicates stronger coupling is that the flux period becomes a rational number, not Φ_0.[25] However, there are instances where the Fermi levels happen to align with an equivalent single loop. The problem is that this may only be true for a single flux value, as opposed to a wide range. This gives little flexibility in trying to meet the other Thévenin requirements such as matching the wavefunctions and transmission in the preserved part of the circuit. Due to this, forming an equivalent model from a network of loops coupled by single paths is not possible.

Since the strongest form of coupled AB rings is ruled out for equivalence, we examine the coupled networks which share two center common paths. While providing two paths for an electron to scatter, the energy levels are altered. In this case, it is not possible to meet all equivalence conditions when the two applied fluxes $\Phi_1 = \Phi_2$. However, an interesting pattern in the band structures for all four classes is found when $\Phi_1 = -\Phi_2$. The Fermi levels for these coupled networks show similarities to a single ring by scaling the value of the electron charge in the ring. In Fig. 6(b), the equivalent Fermi energy region is shown after the electron charge in a single ring is adjusted. Note that when the applied fluxes are opposite in direction, the phase modulation along the center common paths is no longer zero (compared to when the applied fluxes are equal). This leads to a net persistent current flowing in the two common paths and indicates that the band structure must be similar to a single ring (where persistent current is present in all paths).

By considering all possible terminal configurations, the smallest odd $4N+3$ ($M=3$) and even $4N$ ($M=4$) coupled networks are ruled out. While their Fermi levels can be aligned by renormalizing the value of charge in the single rings, the wavefunction distributions do not match for any terminal configuration. However, for the smallest $4N+1$ network ($M=5$), which is larger than the previous two ($M=3$, $M=4$), we can find that all equivalence requirements are satisfied. In the Fig. 6 example, the Fermi levels can be aligned between the coupled network with period $5\Phi_0/6$ and a single $M=5$ ring. The single ring has to be prepared with fractional charge $6e/5$ to yield $\Phi_0' = 5\Phi_0/6$. This allows the Fermi energies to be equal in half of the flux range

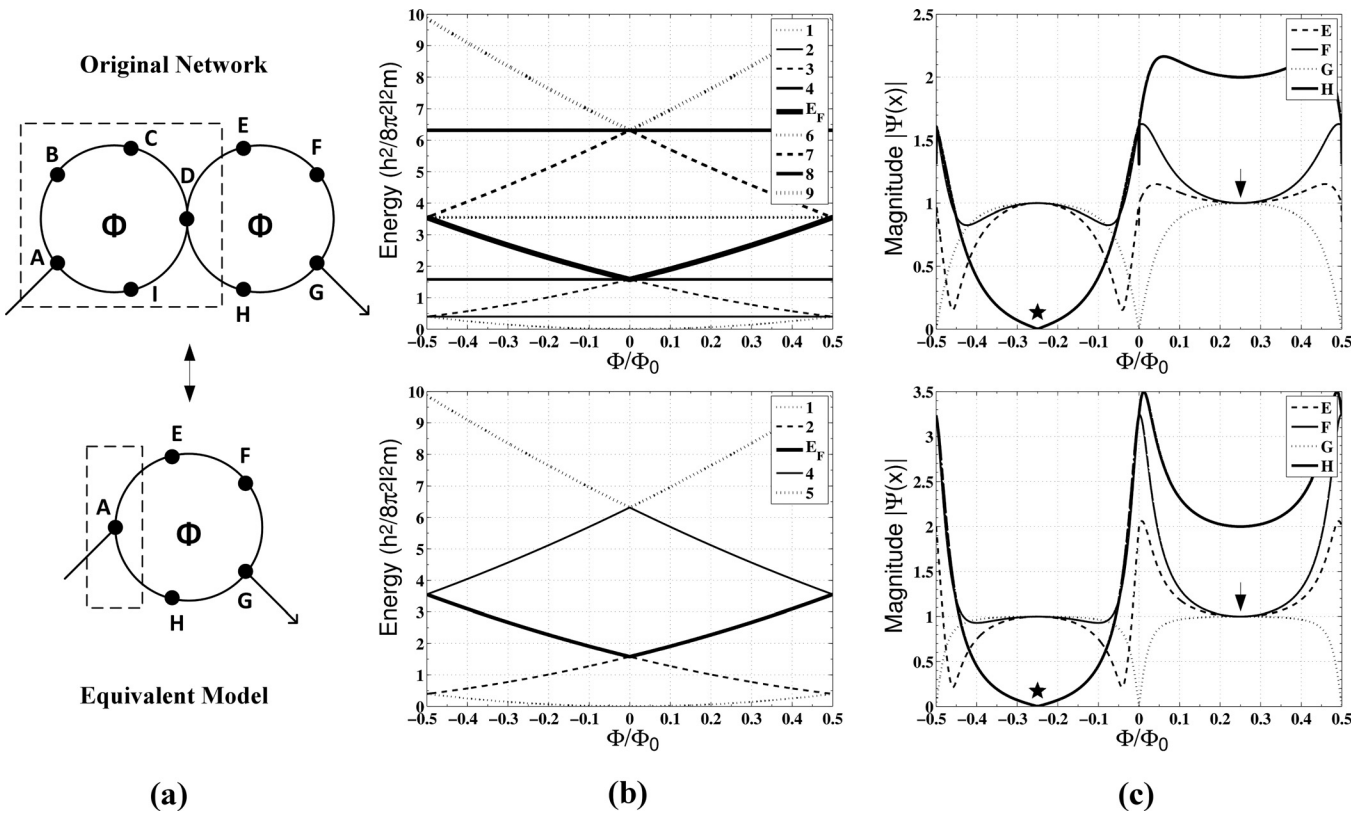

FIG. 5. (a) Diagram of point-contacted $M=5$ loops with an equivalent single ring. (b) Energy band structures (in units of $h^2/8\pi^2 l^2 m$) of both networks computed from their secular determinants, similar to Eq. (5). (c) Wavefunction magnitude for the preserved nodes in each system. The equivalence conditions are only met at two flux values $|\Phi| = \Phi_0/4$, indicated by the pair of arrows and stars, with corresponding energy $E = h^2/32l^2m$. This is because the $\cos kl$ terms vanish in the node equations since the Fermi wavevector $k_F = \pi/2l$. There is a phase difference of $\approx 5/2$ rad between the two networks for both flux values at nodes E, F, G, and H. To obtain complete equivalence, the inputs at A in both networks need to differ by this constant phase.

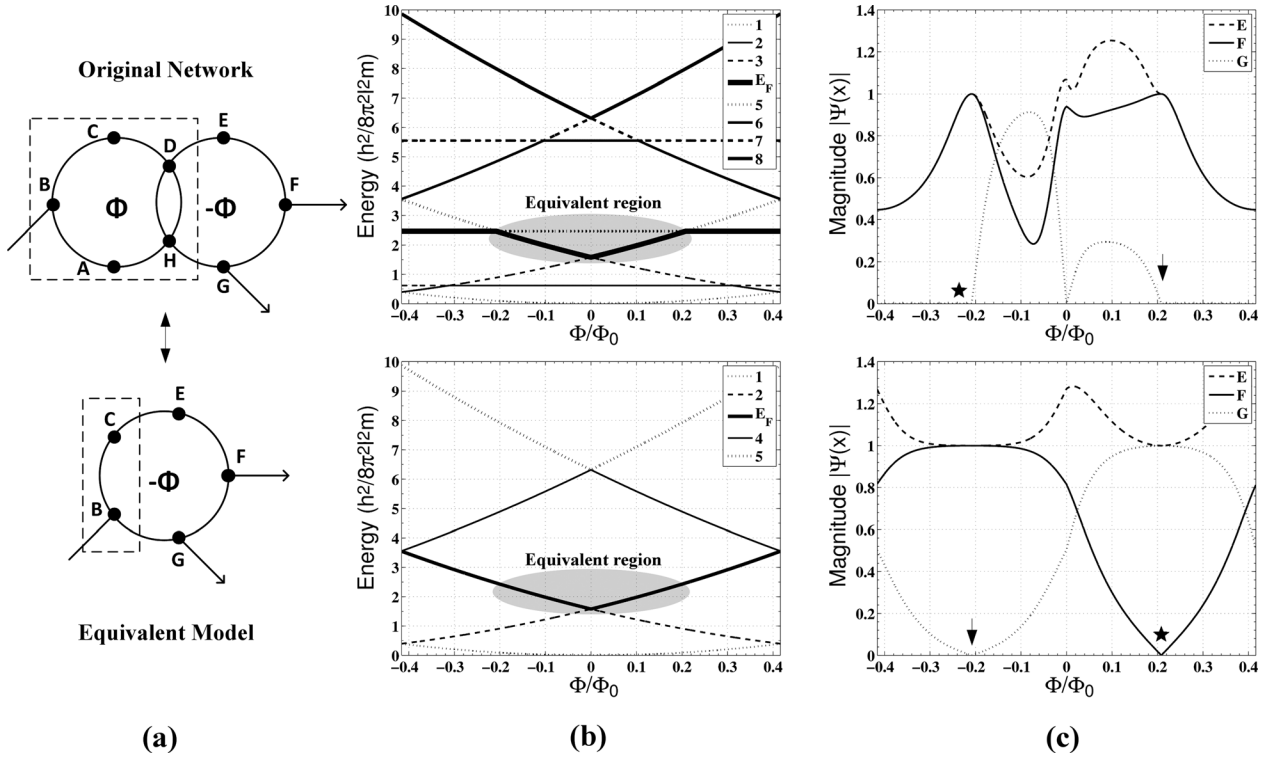

FIG. 6. (a) Diagram of two path coupled $M = 5$ loops with an equivalent single ring. (b) Energy band structures (in units of $h^2/8\pi^2 l^2 m$) of both networks computed from their secular determinants, similar to Eq. (5). The Fermi energies are equivalent in the range $|\Phi| \leq 5\Phi_0/24$, indicated by the shaded region. (c) Wavefunction magnitude for the preserved nodes in each system. All equivalence requirements are satisfied at the two flux values $\pm 5\Phi_0/24$, indicated by the pair of arrows and stars. These points correspond to the same energy as in the point-contact examples, $E = h^2/32l^2m$. This is because the $\cos kl$ terms vanish in the node equations since the Fermi wavevector $k_F = \pi/2l$. The phase difference at nodes E, F, and G between both networks is $\approx \pi^2/4$ rad for the arrow flux values and $\approx 43/64$ rad for the starred values. To obtain complete equivalence, the inputs at B in both networks need to differ by these constant phases.

$|\Phi| \leq 5\Phi_0/24$. If three terminals are attached as shown in Fig. 6(a), an exact equivalence can be achieved at the boundaries of this region $|\Phi| = 5\Phi_0/24$. The transmission circulates between unity at each output, and occurs at the same Fermi wavevector value as the point contact examples discussed previously, $k_F = \pi/2l$. This is not the only viable terminal configuration. By symmetry, one can rearrange the output terminal from G to E while inverting the two flux directions and still satisfy all the equivalence requirements.

The last example is for an even-numbered $4N + 2$ class represented by $M = 6$ and shown in Fig. 7(a), which happens to have particular regions that are able to meet all equivalence conditions. The flux period of this network is $6\Phi_0/7$. A fractional charge of $7e/6$ can be prepared in the single $M = 6$ ring to alter the flux period and align the Fermi energies in the range $6\Phi_0/35 \leq |\Phi| \leq 6\Phi_0/14$ as shown in Fig. 7(b). At the zone boundary $|\Phi| = 6\Phi_0/14$, both networks fully transport through terminal G. Note that the boundary of the equivalent network portion could be extended to include nodes F and I if desired. The Fermi energy and wavevector are consistent with the same values found in all the other examples presented. This is clearly an interesting observation.

IV. CONCLUSION

We have shown that there are possibilities to extend Thévenin's theorem for classical electric circuits into the quantum network regime. For an equivalence to be valid, the node equations for both networks need to be identical in the unaltered part of the circuit. The requirements dictate that the two equivalent networks need to have the same Fermi energies, attributable to the specific structures and applied fluxes involved. In order for the band structures of two networks to be equivalent, and hence suitable for such a transformation, there needs to be some form of symmetry or scaling relation between the two respective networks. This requires the same lattice spacing in both structures. We began with the concept of a single ring being scaled, known to be valid from prior work. The idea was then extended to the four basic AB ring classes, $M = 4N$, $4N + 1$, $4N + 2$, and $4N + 3$, at point-contact coupling. These networks share identical band structures with that of a single ring of the same class but with extra flux invariant states added. With the ability to look for an equivalence across the entire flux period, several examples were identified. Only two classes of rings exist where Thévenin's principle can be applied, when $M = 4N + 1$ or $4N + 3$. For the even-numbered classes, the Fermi energy levels are flux invariant. There is total reflection for any input, making it impossible to find an equivalent network. The Thévenin equivalent is valid up to where the inputs can differ by a constant phase factor. If two point-contacted loops can satisfy all Thévenin requirements, then it is reasonable to assume this can be extended to an arbitrarily large number of point-contacted loops. This would

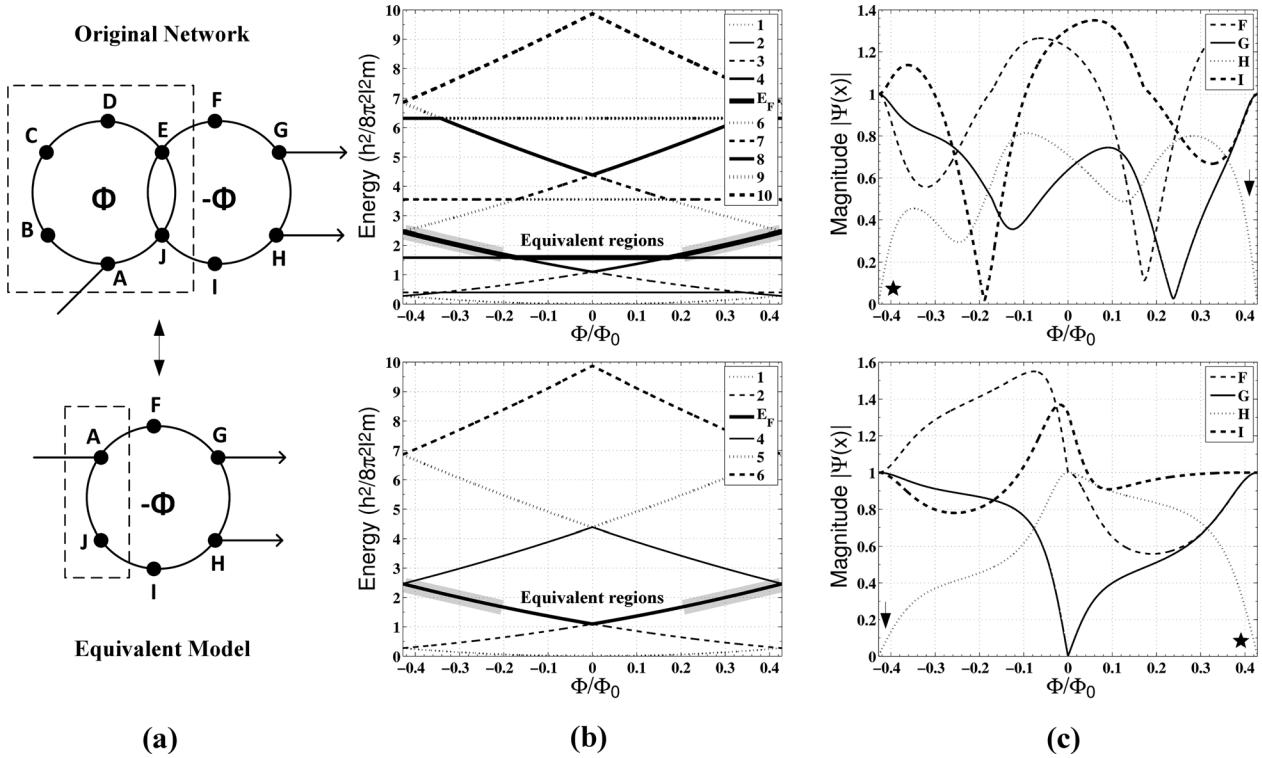

FIG. 7. (a) Diagram of two path coupled $M = 6$ loops with an equivalent single ring. (b) Energy band structures (in units of $h^2/8\pi^2 l^2 m$) of both networks computed from their secular determinants, similar to Eq. (5). The Fermi energies are equivalent between $6\Phi_0/35 \leq |\Phi| \leq 6\Phi_0/14$, indicated by the two shaded regions. (c) Wavefunction magnitude for the preserved nodes in each system. At the zone boundary, all equivalence conditions are met, which like the other examples corresponds to energy $E = h^2/32l^2m$. This is because the $\cos kl$ terms vanish in the node equations since the Fermi wavevector $k_F = \pi/2l$. The phase difference at nodes F, G, H and I between both networks is ≈ 2 rad for the arrow flux values and $\approx 15/8$ rad for the starred values. To obtain complete equivalence, the inputs at A in both networks need to differ by these constant phases.

simply reduce the valid flux range consistent with multistage resonant tunneling.

We further investigated the four classes of coupled AB rings with varying coupling strengths. Two cases are presented: a single path (strongest) and a weaker double path. For double paths, the entanglement of the loops is still weak enough that the band structure is similar to a single ring if the two fluxes are opposite in direction. If the fluxes are equal, there will be no net persistent current flowing in the shared center path, indicating that the band structure will vary too greatly from the single ring spectrum. This kind of coupling changes the flux period to be a fraction of Φ_0. To have any potential Thévenin equivalence, the Fermi level needs to be aligned with that of a single ring. To achieve this, there must be a charge renormalization ($e \rightarrow 7e/6$, as an example). Only two suitable classes exist that meet all of the equivalence requirements. They are the odd-numbered $4N + 1$ and even-numbered $4N + 2$ classes. Consistent with the point-contact cases, the equivalence is only valid at specific flux values and only for a few select terminal configurations. In the valid instances presented, the Fermi energy is $h^2/32l^2m$ with wavevector $\pi/2l$. This leads to vanishing $\cos kl$ terms in the node equations for each network. The result is a simpler set of relations that allow for an equivalence to be obtained.

In summary, the possibility to extend Thévenin's equivalence principle to the mesoscopic regime is limited to specific circumstances, as one would expect. Here, we have outlined what general requirements need to be met. For there to be any possibility of reducing a complex network, the coupling strength between loops formed needs to be weak. When the coupling becomes too strong, the band structure is distorted away from that of a single ring. This then eliminates any possibility of equivalence. With weaker coupling, there are class and terminal restrictions to meet the necessary conditions. In this work, we have focused on exploring these restrictions and providing examples that demonstrate the principle. For any general quantum network, an equivalence may be possible if the portion of the network to be replaced has weak coupling and no disorder.

[1]A. Tonomura, N. Osakabe, T. Matsuda, T. Kawasaki, and J. Endo, Phys. Rev. Lett. **56**, 792 (1986).
[2]S. Washburn and R. A. Webb, Adv. Phys. **35**, 375 (1986).
[3]H. Ajiki and T. Ando, Physica B **201**, 349 (1994).
[4]A. Tonomura, Proc. Jpn. Acad. Ser. B: Phys. Biol. Sci. **82**, 45 (2006).
[5]X. C. Xie and S. D. Sarma, Phys. Rev. B **36**, 9326 (1987).
[6]R. A. Webb, S. Washburn, C. P. Umbach, and R. B. Laibowitz, Phys. Rev. Lett. **54**, 2696 (1985).
[7]N. Byers and C. N. Yang, Phys. Rev. Lett. **7**, 46 (1961).
[8]E. Montroll, J. Math. Phys. **11**, 635 (1970).
[9]S. Alexander, Phys. Rev. B **27**, 1541 (1983).
[10]M. Büttiker, Y. Imry, and M. Y. Azbel, Phys. Rev. A **30**, 1982 (1984).
[11]M. Büttiker, Y. Imry, and R. Landauer, Phys. Lett. **96A**, 365 (1983).
[12]R. Landauer and M. Büttiker, Phys. Rev. Lett. **54**, 2049 (1985).
[13]J. Splettstoesser, M. Governale, and U. Zülicke, Phys. Rev. B **68**, 165341 (2003).
[14]M. Dey, S. K. Maiti, and S. N. Karmakar, J. Appl. Phys. **109**, 024304 (2011).

[15]R. Jackiw, A. I. Milstein, S. Y. Pi, and I. S. Terekhov, Phys. Rev. B **80**, 033413 (2009).
[16]Z. Li and L. R. Ram-Mohan, J. Appl. Phys. **114**, 164322 (2013).
[17]F. Chi and J. Zheng, Appl. Phys. Lett. **92**, 062106 (2008).
[18]M. W. Wu, J. Zhou, and Q. W. Shi, Appl. Phys. Lett. **85**, 1012 (2004).
[19]C. Jiang, W.-J. Gong, and G.-Z. Wei, J. Appl. Phys. **111**, 054306 (2012).
[20]W. Gong, H. Li, S. Zhang, and G. Wei, J. Appl. Phys. **109**, 074315 (2011).
[21]E. R. Hedin and Y. S. Joe, J. Appl. Phys. **110**, 026107 (2011).
[22]F. Chi, J.-L. Liu, and L.-L. Sun, J. Appl. Phys. **101**, 093704 (2007).
[23]J. Chen, M. B. Abdul Jalil, and S. Ghee Tan, J. Appl. Phys. **113**, 17C506 (2013).
[24]L. Diago-Cisneros and F. Mireles, J. Appl. Phys. **114**, 193706 (2013).
[25]C. A. Cain and C. H. Wu, J. Appl. Phys. **110**, 054315 (2011).
[26]C. H. Wu, L. Tran, and C. A. Cain, J. Appl. Phys. **111**, 094304 (2012).
[27]C. A. Cain and C. H. Wu, J. Appl. Phys. **113**, 154309 (2013).
[28]L. Thévenin, Ann. Télégraphiques (Troisieme série) **10**, 222 (1883).
[29]C. Wu and C. Cain, Physica E **59**, 243 (2014).
[30]M. Büttiker, Phys. Rev. Lett. **57**, 1761 (1986).
[31]M. Büttiker, IBM J. Res. Dev. **32**, 317 (1988).
[32]C. H. Wu and G. Mahler, Phys. Rev. B **43**, 5012 (1991).
[33]C. H. Wu and D. Ramamurthy, Phys. Rev. B **65**, 075313 (2002).
[34]D. Ramamurthy and C. H. Wu, Phys. Rev. B **66**, 115307 (2002).